

Four-nucleon scattering: *ab initio* calculations in momentum space

A. Deltuva* and A. C. Fonseca

Centro de Física Nuclear da Universidade de Lisboa, P-1649-003 Lisboa, Portugal

(Received November 9, 2006)

The four-body equations of Alt, Grassberger and Sandhas are solved for n - ${}^3\text{H}$ scattering at energies below three-body breakup threshold using various realistic interactions including one derived from chiral perturbation theory. After partial wave decomposition the equations are three-variable integral equations that are solved numerically without any approximations beyond the usual discretization of continuum variables on a finite momentum mesh. Large number of two-, three- and four-nucleon partial waves are considered until the convergence of the results is obtained. The total n - ${}^3\text{H}$ cross section data in the resonance region is not described by the calculations which confirms previous findings by other groups. Nevertheless the numbers we get are slightly higher and closer to the data than previously found and depend on the choice of the two-nucleon potential. Correlations between the A_y deficiency in n - d elastic scattering and the total n - ${}^3\text{H}$ cross section are studied.

PACS numbers: 21.45.+v, 21.30.-x, 24.70.+s, 25.10.+s

I. INTRODUCTION

The four-nucleon ($4N$) scattering problem gives rise to the simplest set of nuclear reactions that shows the complexity of heavier systems. The neutron- ${}^3\text{H}$ (n - ${}^3\text{H}$) and proton- ${}^3\text{He}$ (p - ${}^3\text{He}$) scattering is dominated by the total isospin $\mathcal{T} = 1$ states while deuteron-deuteron (d - d) scattering by the $\mathcal{T} = 0$ states; the reactions n - ${}^3\text{He}$ and p - ${}^3\text{H}$ involve both $\mathcal{T} = 0$ and $\mathcal{T} = 1$ and are coupled to d - d in $\mathcal{T} = 0$. Due to the charge dependence of the hadronic and electromagnetic interaction a small admixture of $\mathcal{T} = 2$ states is also present. In $4N$ scattering the Coulomb interaction is paramount not only to treat p - ${}^3\text{He}$ but also to separate the n - ${}^3\text{He}$ threshold from p - ${}^3\text{H}$ and at the same time avoid a second excited state of the α particle a few keV below the lowest scattering threshold. All these complex features make the $4N$ scattering problem not only a natural theoretical laboratory to test different force models of the nuclear interaction, but also the next step in the pursuit of very accurate *ab initio* calculations of the N -body scattering problem after the extensive work on the three-nucleon ($3N$) system that has taken place in the past twenty years by several groups [1, 2, 3].

In Refs. [4, 5] all the reactions mentioned above were studied in the framework of Alt, Grassberger, and Sandhas (AGS) equations [6] using the rank one representation of realistic two-nucleon ($2N$) force models together with a high rank representation of all $3N$ subsystem amplitudes; the Coulomb interaction was neglected. This led to one-variable integral equations whose predictive power was limited to the quality of the involved approximations. The calculations showed large discrepancies with data, namely nucleon analyzing power A_y in n - ${}^3\text{He}$ scattering, tensor observables in ${}^2\text{H}(\vec{d}, n){}^3\text{He}$ and ${}^2\text{H}(\vec{d}, d){}^2\text{H}$ and the differential cross section for

${}^2\text{H}(d, n){}^3\text{He}$, but one surprising success in describing the total cross section σ_t for n - ${}^3\text{H}$ scattering in the resonance region where at neutron lab energy $E_n \simeq 3.5$ MeV σ_t rises to about 2.45 b [7]. Calculations by the Grenoble group [8] using coordinate-space solutions of the Faddeev-Yakubovsky equations [9] showed, on the contrary, that realistic interactions missed the total cross section peak by at least 0.2 b. Although these calculations carried out no approximation on the treatment of the $2N$ interaction, they were limited vis-à-vis Ref. [4] on the number of $3N$ and $4N$ partial waves.

Although the issue was recently clarified [10, 11] by comparing to an independent calculation by the Pisa group that uses the Kohn variational method, together with hyperspherical harmonics, further studies based on the AGS equations are needed to settle this important problem because some of the results by the Grenoble and Pisa groups may be still of limited accuracy given the number of included $2N$, $3N$, and $4N$ partial waves. Further investigations are also needed for the understanding of other $4N$ reactions such as p - ${}^3\text{He}$, n - ${}^3\text{He}$ and d - d where large discrepancies with data were previously found. One fundamental issue underlying four-nucleon physics is the existence of correlations between $3N$ and $4N$ observables. One of the best known is the Tjon line [12] which correlates the binding energies of ${}^3\text{H}$ with ${}^4\text{He}$; another one involves the triton binding energy and the singlet (triplet) n - ${}^3\text{H}$ scattering length [13]. Nevertheless, other correlations may exist: one could ask if the persistent A_y problem in n - d scattering is in any way related to the failure to reproduce σ_t in n - ${}^3\text{H}$ scattering in the resonance region, or to the A_y problem in p - ${}^3\text{He}$ [14]; does resolving the former also solves the latter?

Therefore we present here a new numerical approach to the solution of the AGS equations that is both numerically exact and extremely fast in terms of CPU-time demand. Since the $2N$ transition matrix (t -matrix) is treated exactly, the equations we solve are, after partial wave decomposition, three-variable integral equations. The three Jacobi momentum variables in $1+3$ and $2+2$

*Electronic address: deltuv@ci.fc.ul.pt

configurations are discretized on a finite mesh and the number of $2N$, $3N$ and $4N$ partial waves increased up to what is needed for the full convergence of the observables. The present approach also allows for the inclusion of charge-dependent interactions as well as Δ degrees of freedom that lead to an effective $3N$ force. Furthermore, using the method recently proposed to treat the Coulomb force in p - d elastic scattering and breakup [15, 16, 17], we have already obtained preliminary results for p - ^3He elastic scattering observables [18] with the Coulomb potential between the three protons included.

In Sec. II we discuss the integral equations we solve for n - ^3H scattering and in Sec. III we show the results of our most complete calculations, leaving tests of benchmark to the Appendix. Finally conclusions come in Sec. IV.

II. EQUATIONS

As initially proposed by Alt, Grassberger and Sandhas [6] and later reviewed for the purpose of practical applications in Ref. [19], the four-particle scattering equations may be written in a matrix form

$$\mathcal{U} = \mathcal{V} + \mathcal{V} \mathcal{G}_0 \mathcal{U}, \quad (1a)$$

$$\mathcal{U} |\Phi_{\rho_0}\rangle = \mathcal{V} |\Psi_{\rho_0}\rangle, \quad (1b)$$

$$|\Psi_{\rho_0}\rangle = |\Phi_{\rho_0}\rangle + \mathcal{G}_0 \mathcal{V} |\Psi_{\rho_0}\rangle, \quad (1c)$$

where $|\Phi_{\rho_0}\rangle$ is the initial channel state, $|\Psi_{\rho_0}\rangle$ the full scattering state, and ρ_0 defines the two-body entrance channel. Both of them have 18 components, and the transition operator \mathcal{U} as well as \mathcal{V} and \mathcal{G}_0 are 18×18 matrix operators with components

$$[\mathcal{V}]_{ij}^{\sigma\rho} = (G_0 t_i G_0)^{-1} \bar{\delta}_{\sigma\rho} \delta_{ij}, \quad (2a)$$

$$[\mathcal{G}_0]_{ij}^{\sigma\rho} = G_0 t_i G_0 U_{ij}^\sigma G_0 t_j G_0 \delta_{\sigma\rho}. \quad (2b)$$

As usual, $\sigma(\rho)$ denotes two-cluster partitions of $1+3$ or $2+2$ type and $i(j)$ the pair interactions. G_0 is the four free particle Green's function, t_i is the two-particle t-matrix embedded in four-particle space, $\bar{\delta}_{\sigma\rho} = 1 - \delta_{\sigma\rho}$, and U_{ij}^σ are the subsystem transition operators

$$U_{ij}^\sigma = G_0^{-1} \bar{\delta}_{ij} + \sum_k \bar{\delta}_{ki} t_k G_0 U_{kj}^\sigma \quad (3)$$

of $1+3$ or $2+2$ type, depending on σ . If σ is a $1+3$ partition, U_{ij}^σ corresponds to the usual AGS transition matrix for the three interacting particles that are internal to σ . For σ of $2+2$ type U_{ij}^σ does not correspond to any physical process. The components of the initial/final two-cluster states $[\Phi_{\rho_0}]_i^\rho = |\phi_i^{\rho_0}\rangle \delta_{\rho\rho_0}$ are the Faddeev components of the cluster bound state wave function times a plane wave of momentum \mathbf{p}_{ρ_0} between clusters whose dependence is suppressed in our notation,

$$|\phi_i^{\rho_0}\rangle = G_0 t_i \sum_k \bar{\delta}_{ki} |\phi_k^{\rho_0}\rangle. \quad (4)$$

The great advantage of AGS equations over the Yakubovsky equations is that on-shell matrix elements of \mathcal{U} between initial $|\Phi_{\rho_0}\rangle$ and final $|\Phi_{\sigma_0}\rangle$ states with relative two-cluster momenta \mathbf{p}_{ρ_0} and \mathbf{p}'_{σ_0} lead automatically to the corresponding scattering amplitudes

$$\langle \mathbf{p}'_{\sigma_0} | T^{\sigma_0 \rho_0} | \mathbf{p}_{\rho_0} \rangle = \langle \Phi_{\sigma_0} | \mathcal{U} | \Phi_{\rho_0} \rangle \quad (5a)$$

$$= \sum_{ij} \langle \phi_j^{\sigma_0} | \mathcal{U}_{ji}^{\sigma_0 \rho_0} | \phi_i^{\rho_0} \rangle. \quad (5b)$$

For four identical particles the AGS equations reduce to 2×2 matrix equations since there are only two distinct partitions, one of $1+3$ type and one of $2+2$ type, which we choose to be $(12,3)4$ and $(12)(34)$; in the following we denote them by $\alpha = 1$ and $\alpha = 2$, respectively. In this case the equations may be conveniently written using the permutation operators P_{ab} of particles a and b as it was done first in Refs. [20, 21] for the four-nucleon bound state. After the symmetrization of the four-nucleon scattering equations (1) we obtain equations of the same form but with new definitions for the symmetrized operators

$$\mathcal{V}^{\alpha\beta} = (G_0 t G_0)^{-1} (\bar{\delta}_{\alpha\beta} - \delta_{\beta 1} P_{34}), \quad (6a)$$

$$\mathcal{G}_0^{\alpha\beta} = G_0 t G_0 U^\alpha G_0 t G_0 \delta_{\alpha\beta}. \quad (6b)$$

Here t is the pair (12) t-matrix, U^α the symmetrized $1+3$ or $2+2$ subsystem transition operators

$$U^\alpha = P_\alpha G_0^{-1} + P_\alpha t G_0 U^\alpha, \quad (7)$$

and P_α the permutation operators given by

$$P_1 = P = P_{12} P_{23} + P_{13} P_{23}, \quad (8a)$$

$$P_2 = \tilde{P} = P_{13} P_{24}. \quad (8b)$$

The basis states are antisymmetric under exchange of two particles in subsystem (12) for $1+3$ partition and in (12) and (34) for $2+2$ partition. The symmetrized initial/final two-cluster state components are

$$|\phi^\beta\rangle = G_0 t P_\beta |\phi^\beta\rangle. \quad (9)$$

The scattering amplitudes are obtained as

$$\langle \mathbf{p}'_\alpha | T^{\alpha\beta} | \mathbf{p}_\beta \rangle = S_{\alpha\beta} \langle \phi^\alpha | \mathcal{U}^{\alpha\beta} | \phi^\beta \rangle, \quad (10)$$

where $S_{\alpha\beta}$ is a symmetrization factor; $S_{\alpha\alpha} = S_\alpha$ is the number of pairs internal to the partition α , i.e., $S_1 = 3$ and $S_2 = 2$, and $S_{12} = 2S_{21} = 2\sqrt{3}$.

Since the present paper is confined to n - ^3H scattering, we write down explicitly only the equations for the $1+3 \rightarrow 1+3$ and $1+3 \rightarrow 2+2$ transition operators

$$\begin{aligned} \mathcal{U}^{11} = & - (G_0 t G_0)^{-1} P_{34} - P_{34} U^1 G_0 t G_0 \mathcal{U}^{11} \\ & + U^2 G_0 t G_0 \mathcal{U}^{21}, \end{aligned} \quad (11a)$$

$$\begin{aligned} \mathcal{U}^{21} = & (G_0 t G_0)^{-1} (1 - P_{34}) + (1 - P_{34}) U^1 G_0 t G_0 \mathcal{U}^{11}. \end{aligned} \quad (11b)$$

The equations coupling \mathcal{U}^{12} and \mathcal{U}^{22} share an identical kernel but different inhomogeneous terms.

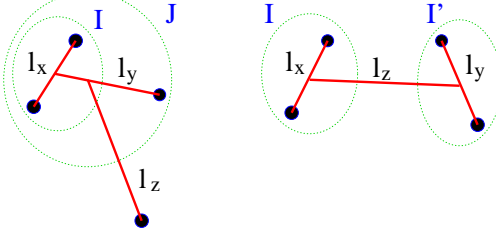


FIG. 1: (Color online) Angular momentum quantum numbers for $1+3$ and $2+2$ basis states.

After the partial wave expansion Eqs. (11) form a set of coupled integral equations with three variables corresponding to the Jacobi momenta k_x , k_y and k_z ; the associated orbital angular momenta are denoted by l_x , l_y , and l_z , respectively. They are depicted in Fig. 1 for $1+3$ and $2+2$ configurations together with the pair total angular momentum I and the three-particle subsystem total angular momentum J . The states of total angular momentum \mathcal{J} are defined as $|k_x k_y k_z [l_z \{l_y [(l_x S_x) I s_y] S_y\} J s_z] \mathcal{J} \mathcal{M}\rangle$ for the $1+3$ configuration and $|k_x k_y k_z (l_z \{l_x S_x\} I [l_y (s_y s_z) S_y] I' S_z) \mathcal{J} \mathcal{M}\rangle$ for the $2+2$, where s_y and s_z are the spins of nucleons 3 and 4, and S_x , S_y , and S_z are channel spins of two-, three-, and four-particle system. In all calculations I and I' run over the same set of quantum numbers.

By the discretization of the momentum variables the integral equations may be turned into a system of linear equations but the direct solution is not possible because of the huge dimension. Therefore, in close analogy with three-nucleon scattering, we calculate the Neumann series for the on-shell matrix elements of the transition operators (11) and sum by the Padé method [22]. The Padé summation algorithm we use is described in Ref. [23]. We work with the half-shell transition operators in the form

$$|X_{\alpha\beta}\rangle = G_0 \mathcal{U}^{\alpha\beta} |\phi^\beta\rangle \quad (12)$$

such that the on-shell elements are $\langle \phi^\alpha | \mathcal{U}^{\alpha\beta} | \phi^\beta \rangle = \langle \xi_\alpha | X_{\alpha\beta} \rangle$ with the auxiliary states $|\xi_\alpha\rangle = G_0^{-1} |\phi^\alpha\rangle = t P_\alpha |\phi^\alpha\rangle$. Defining $Q_\alpha = G_0 U^\alpha G_0 t$ and using Eq. (9) for the inhomogeneous terms in order to eliminate $(G_0 t G_0)^{-1}$, Eqs. (11) become

$$|X_{11}\rangle = -P_{34} P_1 G_0 |\xi_1\rangle - P_{34} Q_1 |X_{11}\rangle + Q_2 |X_{21}\rangle, \quad (13a)$$

$$|X_{21}\rangle = (1 - P_{34}) P_1 G_0 |\xi_1\rangle + (1 - P_{34}) Q_1 |X_{11}\rangle. \quad (13b)$$

In practical calculations, in order to accelerate the convergence of the Padé summation, it is advantageous to substitute Eq. (13b) into Eq. (13a) yielding the Neumann

series

$$|X_{\alpha\beta}\rangle = \sum_{n=0}^{\infty} |X_{\alpha\beta}^{(n)}\rangle, \quad (14a)$$

$$|X_{21}^{(0)}\rangle = (1 - P_{34}) P_1 G_0 |\xi_1\rangle, \quad (14b)$$

$$|X_{11}^{(0)}\rangle = -P_{34} P_1 G_0 |\xi_1\rangle + Q_2 |X_{21}^{(0)}\rangle, \quad (14c)$$

$$|X_{21}^{(n)}\rangle = (1 - P_{34}) Q_1 |X_{11}^{(n-1)}\rangle, \quad (14d)$$

$$|X_{11}^{(n)}\rangle = -P_{34} Q_1 |X_{11}^{(n-1)}\rangle + Q_2 |X_{21}^{(n)}\rangle, \quad (14e)$$

which requires $1+3$ and $2+2$ subsystem transition operators U^α , contained in Q_α , fully off-shell at different energies. Explicit calculation of U^α is not only very time consuming but also requires large storage devices. Therefore, except at the bound state poles, we do not calculate the full off-shell transition matrices U^α explicitly. Instead, we rewrite Eq. (7) as a Neumann series

$$U^\alpha = \sum_{r=0}^{\infty} (P_\alpha t G_0)^r P_\alpha G_0^{-1} \quad (15)$$

resulting a corresponding Neumann series for the solution vectors in Eqs. (14), i.e.,

$$Q_\alpha |X_{\alpha\beta}^{(n)}\rangle = \sum_{r=1}^{\infty} |X_{\alpha\beta}^{(n,r)}\rangle, \quad (16a)$$

$$|X_{\alpha\beta}^{(n,0)}\rangle = |X_{\alpha\beta}^{(n)}\rangle, \quad (16b)$$

$$|X_{\alpha\beta}^{(n,r)}\rangle = P_\alpha G_0 t |X_{\alpha\beta}^{(n,r-1)}\rangle, \quad (16c)$$

where the summation again has to be performed using the Padé method. Usually, 6 to 18 Padé iteration steps are required for the convergence in Eqs. (14) - (16). At the bound state poles the subsystem transition operators are

$$U^\alpha = P_\alpha |\xi_\alpha\rangle \frac{S_\alpha}{E + i0 - h_0^z - E_B} \langle \xi_\alpha | P_\alpha, \quad (17)$$

where E is the available four-nucleon energy, E_B the binding energy, and h_0^z the kinetic energy operator for the relative motion of the two clusters.

Thus, compared to the calculation of full off-shell U^α , the method we are using avoids storage problems and also significantly reduces the number of required floating point operations, since it is essentially a calculation of *half-shell* matrix elements for a number of driving terms that are considerably fewer than the linear dimension of the discretized U^α . A further advantage is that the matrices corresponding to the operators P_α , G_0 and t in Eq. (16c) have block-diagonal structure whereas U^α is a full matrix.

The calculation of the Neumann series (16) for $\alpha = 1$ is what we are doing in three-nucleon scattering and is described in great detail in Refs. [24, 25]. The specific representation of the permutation operator P_1 where the initial and final state momenta k_y are chosen as independent variables requires the interpolation in the momentum k_x for the quantities on both sides of $P_1 G_0$, i.e., for

t or $\langle \xi_\alpha \rangle$. Two interpolation methods using Chebyshev polynomials and spline functions were used in Ref. [24]; in the context of four-nucleon equations where one has to work with $1+3$ and $2+2$ basis states the spline interpolation is more convenient.

The calculation of the Neumann series (16) for $\alpha = 2$ is straightforward because of the very simple form of the permutation operator P_2 .

Finally, the application of the permutation operator P_{34} as well as the transformation of $|X_{\alpha\beta}^{(n)}\rangle$ from $1+3$ basis to $2+2$ or vice versa has a structure similar to that of P_1 , resulting in a similar treatment. The specific representation of P_{34} , i.e.,

$$\begin{aligned} \langle k_x k_y k_z | P_{34} | k'_x k'_y k'_z \rangle &= \frac{\delta(k_x - k'_x)}{k_x^2} \int_{-1}^1 dy P_{34}(k_z, k'_z, y) \\ &\times \frac{\delta(k_y - \bar{k}_y(k_z, k'_z, y))}{k_y^2} \\ &\times \frac{\delta(k'_y - \bar{k}'_y(k_z, k'_z, y))}{k'_y^2}, \end{aligned} \quad (18)$$

where the initial and final state momenta k_z are chosen as independent variables, requires the interpolation in the momentum k_y for the quantities on both sides of P_{34} that are calculated on the mesh $\{k_{i_y}\}$. The dependence on the discrete quantum numbers is suppressed since it is irrelevant for the consideration as well as the explicit form of function $P_{34}(k_z, k'_z, y)$. $\bar{k}_y(k_z, k'_z, y)$ and $\bar{k}'_y(k_z, k'_z, y)$ are the initial and final state Jacobi momenta k_y expressed via k'_z , k_z , and the angle between them $y = \hat{k}'_z \cdot \hat{k}_z$. We use the spline interpolation again with the spline functions $S_{i_y}(k)$ [26, 27, 28] such that for the function $f(k)$, given on the mesh $\{k_{i_y}\}$, the values at any k may be obtained by

$$f(k) \approx \sum_{i_y} f(k_{i_y}) S_{i_y}(k). \quad (19)$$

For P_{34} acting on the vector $|Y\rangle$ we obtain the following result (as a distribution)

$$\begin{aligned} \langle k_x k_y k_z | P_{34} | Y \rangle &= \sum_{i_y} \frac{\delta(k_y - k_{i_y})}{k_y^2} \int_0^\infty k'_z^2 dk'_z \int_{-1}^1 dy \\ &\times S_{i_y}(\bar{k}_y(k_z, k'_z, y)) P_{34}(k_z, k'_z, y) \\ &\times \sum_{j_y} S_{j_y}(\bar{k}'_y(k_z, k'_z, y)) \langle k_x k_{j_y} k'_z | Y \rangle \\ &= \sum_{i_y} \frac{\delta(k_y - k_{i_y})}{k_y^2} \tilde{Y}_{i_y}(k_x, k_z), \end{aligned} \quad (20)$$

such that in the next step of the calculation, where the $\langle k_x k_y k_z | P_{34} | Y \rangle$ has to be multiplied by a smooth function $f(k_y)$ and integrated over k_y , the result simply is the sum

over the meshpoints $\{k_{i_y}\}$ for the involved quantities,

$$\int_0^\infty k_y^2 dk_y f(k_y) \langle k_x k_y k_z | P_{34} | Y \rangle = \sum_{i_y} f(k_{i_y}) \tilde{Y}_{i_y}(k_x, k_z). \quad (21)$$

The integrations in Eq. (20) are performed using Gaussian integration rules [28]. The bound state pole (17) is treated by the subtraction technique much like the deuteron pole in the n - d scattering [24]. Note that the representation of the operators P_1 and P_{34} is different from the one used in Refs. [20, 29] where final state momenta k_y and k_z were chosen as independent variables.

III. RESULTS

In order to calibrate our work we start by reproducing results of previous calculations, in particular the binding energy of ${}^4\text{He}$ obtained with different realistic $2N$ interactions by different groups [10, 29, 30, 31] as well as the n - ${}^3\text{H}$ phase shifts obtained with Mafliet-Tjon potential by the Grenoble group [32]. Furthermore, we check the numerical stability of our calculations. These results are presented in the Appendix and show that the present algorithm is numerically highly reliable and capable of reproducing previous published results.

Next we study the convergence of our calculations in terms of number of $2N$, $3N$, and $4N$ partial waves using the AV18 potential [33] for the $2N$ interaction. In the calculations presented here for the n - ${}^3\text{H}$ scattering we include only the total isospin $\mathcal{T} = 1$ states, but, within $\mathcal{T} = 1$, we take into account all couplings resulting from the charge dependence of the interaction. Including $\mathcal{T} = 2$ states would yield an effect that is of 2nd order in the charge dependence and, therefore, is expected to be extremely small much like the effect of the total $3N$ isospin $T = \frac{3}{2}$ states in elastic n - d scattering. Coupling to $\mathcal{T} = 2$ states is neglected also in all previous calculations, but in configuration-space treatments the isospin averaging within $\mathcal{T} = 1$ states is performed for the potential, whereas we perform it for the t-matrix.

In Table I we show n - ${}^3\text{H}$ phase shifts, 1^- mixing parameter ϵ , and total cross section σ_t at $E_n = 4$ MeV neutron lab energy for increasing number of $2N$ partial waves. In all calculations we keep $l_y, l_z \leq 4$ and $J \leq \frac{9}{2}$. We apply additional restrictions that are different for $1+3$ and $2+2$ states. We include all $1+3$ states with $l_x + l_y \leq 8$ plus the states coupled to them by the tensor force; the above restriction is not applied if $I \leq 2$. We include all $2+2$ states with $l_x + l_y + l_z \leq 10$ plus states coupled to them by the tensor force. One finds that at least $I \leq 3 + {}^3F_4$ is needed for a well converged calculation. Likewise in Table II we show similar results for increasing l_y, l_z keeping $I \leq 4 + {}^3G_5$ and $J \leq \frac{9}{2}$. At least $l_y, l_z \leq 3$ is needed to get quite satisfactorily converged results for the P -wave phase shifts, particularly 3P_2 . Finally in Table III we show results for increasing J , keeping $l_y, l_z \leq 4$

| | $0^+ ({}^1S_0)$ | $0^- ({}^3P_0)$ | $1^+ ({}^3S_1)$ | $1^- ({}^3P_1)$ | $1^- ({}^1P_1)$ | $1^- (\epsilon)$ | $2^- ({}^3P_2)$ | σ_t |
|----------------------|-----------------|-----------------|-----------------|-----------------|-----------------|------------------|-----------------|------------|
| $I \leq 1^+$ | -69.54 | 20.97 | -62.31 | 46.47 | 26.46 | -37.74 | 36.19 | 2.106 |
| $I \leq 1 + {}^3P_2$ | -70.60 | 22.82 | -62.70 | 40.30 | 21.25 | -44.00 | 43.53 | 2.151 |
| $I \leq 2 + {}^3D_3$ | -70.02 | 24.43 | -62.05 | 43.62 | 22.65 | -44.46 | 47.06 | 2.301 |
| $I \leq 3 + {}^3F_4$ | -69.68 | 23.52 | -61.74 | 43.37 | 22.35 | -44.71 | 46.71 | 2.277 |
| $I \leq 4 + {}^3G_5$ | -69.63 | 23.62 | -61.69 | 43.54 | 22.38 | -44.69 | 47.03 | 2.288 |
| $I \leq 5 + {}^3H_6$ | -69.61 | 23.56 | -61.68 | 43.53 | 22.37 | -44.73 | 47.00 | 2.286 |

TABLE I: n^- phase shifts, 1^- mixing parameter ϵ (in degrees) and the total cross section σ_t (in barns) at $E_n = 4$ MeV neutron lab energy for increasing number of $2N$ partial waves and fixed $l_y, l_z \leq 4$, $J \leq \frac{9}{2}$. The $2N$ potential is AV18.

| | $0^+ ({}^1S_0)$ | $0^- ({}^3P_0)$ | $1^+ ({}^3S_1)$ | $1^- ({}^3P_1)$ | $1^- ({}^1P_1)$ | $1^- (\epsilon)$ | $2^- ({}^3P_2)$ | σ_t |
|-------------------|-----------------|-----------------|-----------------|-----------------|-----------------|------------------|-----------------|------------|
| $l_y, l_z \leq 0$ | -69.70 | | -63.50 | | | | | 0.950 |
| $l_y, l_z \leq 1$ | -69.59 | 22.62 | -61.94 | 41.33 | 22.65 | -44.49 | 43.35 | 2.163 |
| $l_y, l_z \leq 2$ | -69.67 | 23.19 | -61.75 | 42.65 | 22.05 | -44.88 | 44.10 | 2.196 |
| $l_y, l_z \leq 3$ | -69.62 | 23.65 | -61.72 | 43.35 | 22.34 | -44.84 | 46.82 | 2.279 |
| $l_y, l_z \leq 4$ | -69.63 | 23.62 | -61.69 | 43.54 | 22.38 | -44.69 | 47.03 | 2.288 |

TABLE II: Same as in Table I for increasing l_y, l_z and fixed $I \leq 4 + {}^3G_5$ and $J \leq \frac{9}{2}$. The restriction on l_y is not applied to $3N$ partial waves with total angular momentum and parity $J^\pi = \frac{1}{2}^+$.

| | $0^+ ({}^1S_0)$ | $0^- ({}^3P_0)$ | $1^+ ({}^3S_1)$ | $1^- ({}^3P_1)$ | $1^- ({}^1P_1)$ | $1^- (\epsilon)$ | $2^- ({}^3P_2)$ | σ_t |
|----------------------|-----------------|-----------------|-----------------|-----------------|-----------------|------------------|-----------------|------------|
| $J \leq \frac{1}{2}$ | -69.84 | 23.95 | -53.98 | 27.53 | 17.55 | -9.48 | 17.56 | 1.268 |
| $J \leq \frac{3}{2}$ | -69.61 | 23.26 | -62.41 | 43.05 | 22.34 | -44.85 | 21.97 | 1.715 |
| $J \leq \frac{5}{2}$ | -69.63 | 23.61 | -61.69 | 43.49 | 22.37 | -44.63 | 46.97 | 2.285 |
| $J \leq \frac{7}{2}$ | -69.63 | 23.61 | -61.69 | 43.53 | 22.38 | -44.68 | 46.99 | 2.287 |
| $J \leq \frac{9}{2}$ | -69.63 | 23.62 | -61.69 | 43.54 | 22.38 | -44.69 | 47.03 | 2.288 |

TABLE III: Same as in Table I for increasing J and fixed $I \leq 4 + {}^3G_5$ and $l_y, l_z \leq 4$.

| | $0^+ ({}^1S_0)$ | $0^- ({}^3P_0)$ | $1^+ ({}^3S_1)$ | $1^- ({}^3P_1)$ | $1^- ({}^1P_1)$ | $1^- (\epsilon)$ | $2^- ({}^3P_2)$ | σ_t |
|-------------|-----------------|-----------------|-----------------|-----------------|-----------------|------------------|-----------------|------------|
| AV18 | -66.12 | 20.75 | -58.48 | 40.09 | 20.73 | -44.50 | 42.51 | 2.331 |
| Ref. [11] | -66.5 | 20.9 | -58.5 | 37.3 | 20.7 | -43.5 | 41.0 | 2.24 |
| Ref. [11] | -66.3 | 20.6 | -58.7 | 38.6 | 20.5 | -45.5 | 40.1 | 2.24 |
| rank 1 | -66.06 | 26.99 | -58.55 | 42.36 | 22.15 | -44.81 | 45.06 | 2.488 |
| CD Bonn | -64.63 | 18.97 | -57.40 | 39.44 | 20.20 | -44.94 | 42.47 | 2.283 |
| Nijmegen I | -65.61 | 19.64 | -58.16 | 39.62 | 20.40 | -44.91 | 42.13 | 2.297 |
| Nijmegen II | -65.98 | 20.02 | -58.42 | 39.69 | 20.44 | -44.71 | 42.22 | 2.308 |
| INOY04 | -62.91 | 16.73 | -56.00 | 38.75 | 19.47 | -44.55 | 42.13 | 2.216 |
| N3LO | -65.54 | 20.31 | -57.99 | 40.94 | 20.74 | -44.71 | 43.98 | 2.377 |

TABLE IV: n^- phase shifts, mixing parameter ϵ , and total cross section σ_t for AV18, CD-Bonn, Nijmegen I, Nijmegen II, INOY04, and N3LO potentials at $E_n = 3.5$ MeV together with results from other calculations for AV18. We include $I \leq 4 + {}^3G_5$, $l_y, l_z \leq 4$, and $J \leq \frac{9}{2}$.

and $I \leq 4 + {}^3G_5$. We find that the inclusion of at least $J = \frac{5}{2}$ $3N$ states is necessary without which A_y has the wrong sign. Compared with previous calculations the present work exceeds in the number of $2N$, $3N$, and $4N$ partial waves included, providing very accurate results

for all observables.

In Table IV we show the results of the other calculations for AV18 at $E_n = 3.5$ MeV which were compiled in Ref. [11]. The present calculation confirms the work of the Grenoble and Pisa groups (second and third

lines, respectively) and clearly shows in the fourth line the shortcomings of the rank one representation of realistic interactions calculated again using the present numerical algorithm. As in the work of Ref. [4] the total cross section gets to be $\sigma_t = 2.49$ b which even slightly overestimates the experimental value. Calculations with other potentials, i.e., charge-dependent (CD) Bonn [34], Nijmegen I and II [35], inside-nonlocal outside-Yukawa (INOY04) potential by Doleschall [10, 36], and the one derived from chiral perturbation theory at next-to-next-to-next-to-leading order (N3LO) [37], show similar results for all phases although N3LO gives the largest P -wave phases leading to $\sigma_t = 2.38$ b, the closest to the experimental value at the resonance peak using two-body interactions alone.

In Fig. 2 we show the total cross section for $n-^3\text{H}$ scattering as a function of the neutron lab energy; for clarity we skip the Nijmegen I and II predictions since they are between AV18 and CD Bonn. In the resonance region all potentials fail to reproduce the experimental data though some do better than others. As pointed out in Ref. [10] the nonlocal potential INOY04 that, by itself alone, leads to the correct triton binding energy and slightly overbinds the α particle, shows the lowest total cross section at the peak. On the contrary CD Bonn and AV18 show higher total cross sections but also lower triton and α particle binding energies.

In Table V we give the values for the triton and α particle binding energies, singlet and triplet scattering lengths a_0 and a_1 , and total cross section at $E_n = 0$ and 3.5 MeV. The results we get for a_0 and a_1 agree with previous work for AV18 [10, 11], and as shown in Fig. 3 correlate with the triton binding energy. Therefore interactions that lead to lower triton binding show the highest values for a_0 and a_1 and consequently the higher total cross sections at threshold. Nevertheless at $E_n = 3.5$ MeV this correlation gets destroyed as the behavior of N3LO shows. Further studies are needed to understand the features of N3LO that give rise to this breaking of the correlation near the peak of the resonance.

| | ε_t | ε_α | a_0 | a_1 | $\sigma_t(0)$ | $\sigma_t(3.5)$ |
|-------------|-----------------|----------------------|-------|-------|---------------|-----------------|
| AV18 | 7.621 | 24.24 | 4.28 | 3.71 | 1.88 | 2.33 |
| Nijmegen II | 7.653 | 24.50 | 4.27 | 3.71 | 1.87 | 2.31 |
| Nijmegen I | 7.734 | 24.94 | 4.25 | 3.69 | 1.85 | 2.30 |
| N3LO | 7.854 | 25.38 | 4.23 | 3.67 | 1.83 | 2.38 |
| CD Bonn | 7.998 | 26.11 | 4.17 | 3.63 | 1.79 | 2.28 |
| INOY04 | 8.493 | 29.11 | 4.02 | 3.51 | 1.67 | 2.22 |

TABLE V: ${}^3\text{H}$ and ${}^4\text{He}$ binding energies ε_t and ε_α (in MeV), $n-{}^3\text{H}$ scattering lengths a_0 and a_1 (in fm), and $n-{}^3\text{H}$ total cross section σ_t (in barns) at $E_n = 0$ and 3.5 MeV neutron lab energy for different $2N$ potentials.

In Fig. 4 we show the differential cross section $d\sigma/d\Omega$ and the neutron analyzing power A_y for $n-{}^3\text{H}$ scattering at neutron lab energies of 1, 2, 3.5, and 6 MeV. In order to

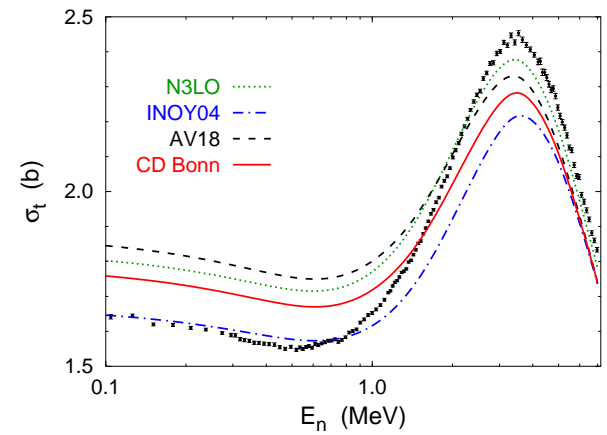


FIG. 2: (Color online) Total cross section for $n-{}^3\text{H}$ scattering as function of neutron lab energy calculated with CD Bonn (solid curve), AV18 (dashed curve), INOY04 (dash-dotted curve), and N3LO (dotted curve) potentials. Experimental data are from Ref. [7].

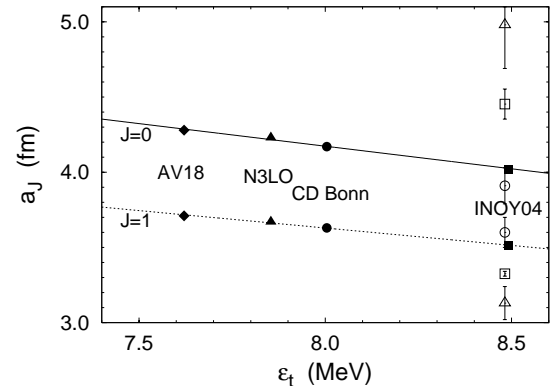


FIG. 3: Correlation between ${}^3\text{H}$ binding energy ε_t and $n-{}^3\text{H}$ scattering lengths a_0 and a_1 . The predictions for AV18 (diamonds), N3LO (triangles), CD Bonn (circles), and INOY04 (squares) are shown. The experimental data are from Ref. [38] (open circles), Ref. [39] (open triangles), and Ref. [40] (open squares).

get fully converged results we take into account all $n-{}^3\text{H}$ channel states with orbital angular momentum $L \leq 3$. The predictions of the four potentials differ mostly at forward and backward angles for the differential cross section and around the peak for the analyzing power. It is not obvious to us that the disagreement with the total cross section data shown in Fig. 2 is compatible with the discrepancies we observe relative to the differential cross section data. Therefore it would be recommended that some of the experiments be repeated at specific energies and A_y measured in order to further understand the implications of the $2N$ force models.

One important observation that comes out of these calculations is the increased sensitivity of $4N$ observables to

changes in the $2N$ interaction. The variations due to the $2N$ potential at the maximum of $n\text{-}{}^3\text{H}$ A_y lead to about 16% fluctuations which are larger than the 10% fluctuations observed at the peak of A_y in low energy $n\text{-}d$ scattering. This indicates that the $4N$ system is more sensitive to off-shell differences of the $2N$ force than the $3N$ system.

Finally, in Table VI we investigate the possible correlations between the A_y -puzzle in low energy $n\text{-}d$ scattering and the underestimation of σ_t in $n\text{-}{}^3\text{H}$ scattering in the resonance region. The experimental data for A_y in $n\text{-}d$ scattering can be accounted for by a calculation with modified interactions in $2N$ 3P_I waves [36, 42]. We use two models. The first one, AV18', is taken from Ref. [42]; it corresponds to the AV18 potential that in 3P_I waves is multiplied by strength factors 0.96, 0.98, and 1.06 for $I = 0, 1$, and 2, respectively. The second one, INOY04', is taken from Ref. [36] and differs from INOY04 by 3P_I wave parameters. Although both modified potentials provide quite satisfactory description of vector analyzing powers in low energy $n\text{-}d$ scattering, they are incompatible with present day $2N$ data basis. E.g., the χ^2/datum values with respect to the pp data, estimated using the Nijmegen error matrix [43], i.e., by comparing to the Nijmegen phase shifts rather than to data directly, are 3.5 for INOY04' and 4.4 for AV18' potentials. However, those modifications of the potentials are unable to resolve the σ_t discrepancy in $n\text{-}{}^3\text{H}$ scattering. The σ_t is slightly increased for AV18' but it gets even lower for INOY04', indicating that σ_t depends on the $2N$ 3P_I wave interaction in a different way than the A_y in the $n\text{-}d$ scattering.

IV. CONCLUSIONS

In the present paper we developed a new numerical approach to solve four-nucleon scattering equations in momentum-space. The method uses no uncontrolled approximations, is numerically very efficient and therefore can include very large number of partial waves, thereby yielding well converged and very precise results. The developed approach is applied to $n\text{-}{}^3\text{H}$ scattering below three-body breakup threshold. The calculations with various realistic $2N$ potentials underestimate the total $n\text{-}{}^3\text{H}$ cross section data in the resonance region as already found by other groups. However, probably due to the inclusion of more partial waves, the numbers we get are slightly higher and closer to the data; they also depend on the choice of the $2N$ potential. The new results also show that $4N$ observables are more sensitive than

$3N$ observables to the off-shell nature of the $2N$ interaction. Furthermore, the modifications that are required to introduce at the level of the 3P_I $2N$ partial waves to remove the discrepancies in $n\text{-}d$ A_y at low energy, do not remove the disagreement observed in the total $n\text{-}{}^3\text{H}$ cross section around $E_n = 3.5$ MeV. Finally, to understand the compatibility between existing $n\text{-}{}^3\text{H}$ total and differential cross section data it would be advisable to repeat some of those experiments at specific energies.

Acknowledgments

The authors thank R. Lazauskas for valuable discussions and for providing benchmark results. A.D. is supported by the Fundação para a Ciência e a Tecnologia (FCT) grant SFRH/BPD/14801/2003 and A.C.F. in part by the FCT grant POCTI/ISFL/2/275.

APPENDIX A

As mentioned in Section III we present here our results for the binding energy of ${}^4\text{He}$ and $n\text{-}{}^3\text{H}$ phase shifts obtained with Mafliet-Tjon potential as well as the numerical stability check of our results. In Table VII we show the α particle binding energy for increasing number of $2N$ partial waves and compare with previous works. Results with AV8' are calculated without the Coulomb interaction in order to compare with Ref. [30]. On the other hand calculations from Ref. [29, 31] with CD Bonn include coupling between total isospin $T = 0, 1$ and 2 states while we consider only $T = 0$. In contrast to our scattering calculations, here we perform the isospin averaging not for the t-matrix but for the potential like it has been done in calculations of Ref. [10]. Overall these results indicate that our algorithm is accurate and reliable.

For $n\text{-}{}^3\text{H}$ scattering we compare in Table VIII the results of our calculations with those of the Grenoble group [32]. Again our phase shifts agree within a few tenth of a degree or better leading to identical total cross sections over a wide range of energies.

In Table IX we demonstrate the stability of our results increasing the number N_k of momentum meshpoints. All calculations use AV18 potential with $2N$ partial waves $I \leq 4 + {}^3G_5$, $l_y, l_z \leq 4$ and $J \leq \frac{9}{2}$. The results with $N_k = 20$ which is the choice for calculations of Tables I — III are converged to better than 0.05 deg for all phase shifts.

[1] W. Glöckle, H. Witała, D. Hüber, H. Kamada, and J. Golak, Phys. Rep. **274**, 107 (1996).
[2] J. Golak, R. Skibiński, H. Witała, W. Glöckle, A. Nogga, and H. Kamada, Phys. Rep. **415**, 89 (2005).
[3] A. Kievsky, M. Viviani, and S. Rosati, Phys. Rev. C **64**, 024002 (2001).

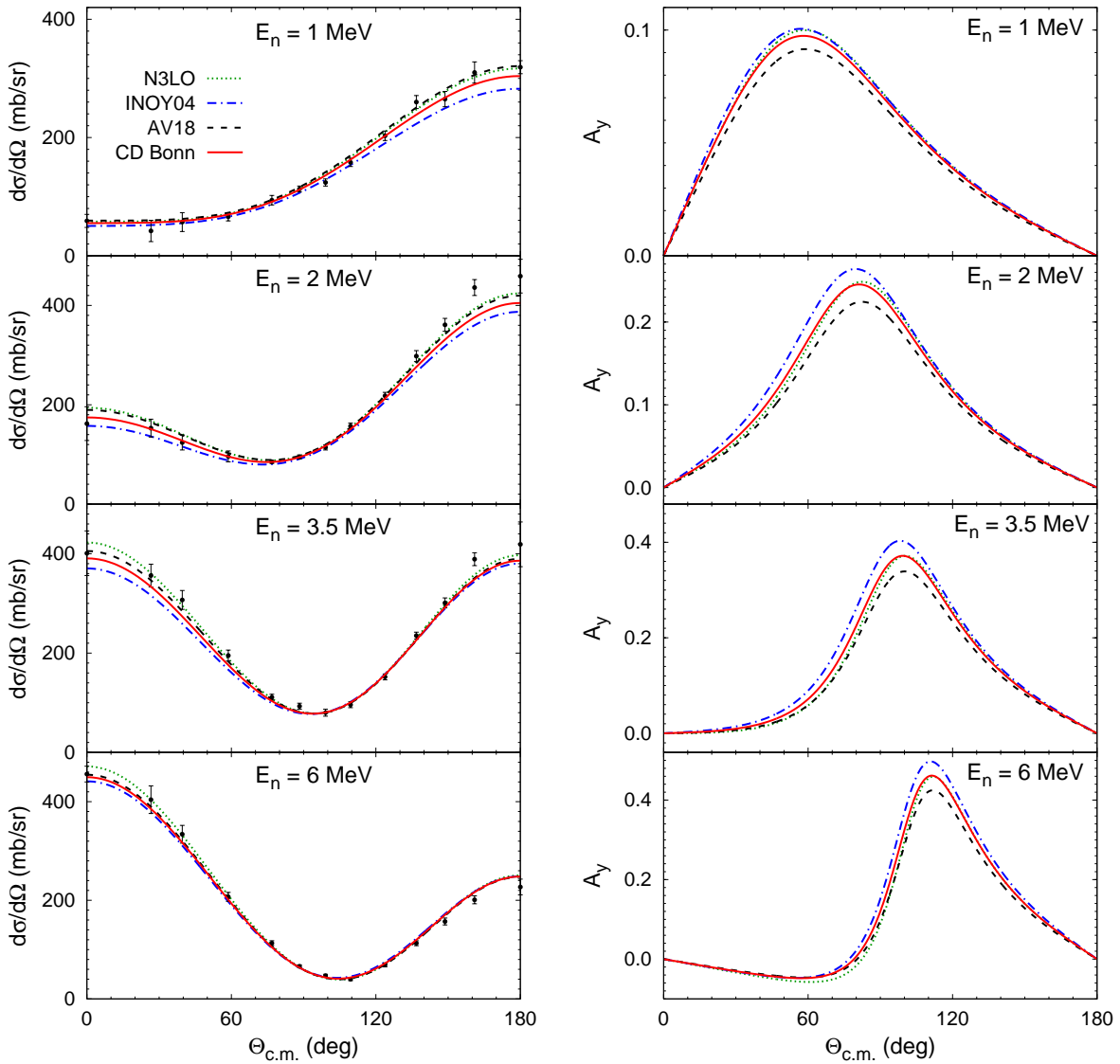


FIG. 4: (Color online) Differential cross section and neutron analyzing power for $n-^3H$ scattering at $E_n = 1, 2, 3.5$, and 6 MeV neutron lab energies as functions of c.m. scattering angle. Curves as in Fig. 2. Experimental data are from Ref. [41].

| | $0^+ (^1S_0)$ | $0^- (^3P_0)$ | $1^+ (^3S_1)$ | $1^- (^3P_1)$ | $1^- (^1P_1)$ | $1^- (\epsilon)$ | $2^- (^3P_2)$ | σ_t |
|---------|---------------|---------------|---------------|---------------|---------------|------------------|---------------|------------|
| AV18 | -66.12 | 20.75 | -58.48 | 40.09 | 20.73 | -44.50 | 42.51 | 2.331 |
| AV18' | -66.06 | 20.46 | -58.39 | 40.50 | 20.86 | -44.70 | 43.82 | 2.375 |
| INOY04 | -62.91 | 16.73 | -56.00 | 38.75 | 19.47 | -44.55 | 42.13 | 2.216 |
| INOY04' | -63.04 | 15.67 | -56.16 | 37.41 | 19.06 | -43.06 | 42.21 | 2.191 |

TABLE VI: $n-^3H$ phase shifts, 1^- mixing parameter ϵ , and total cross section σ_t at $E_n = 3.5$ MeV for original AV18 and INOY04 potentials and their versions AV18' and INOY04' with modified P -waves.

- [4] A. C. Fonseca, Phys. Rev. Lett. **83**, 4021 (1999).
- [5] A. C. Fonseca, G. Hale, and J. Haidenbauer, Few-Body Syst. **31**, 139 (2002).
- [6] P. Grassberger and W. Sandhas, Nucl. Phys. **B2**, 181 (1967); E. O. Alt, P. Grassberger, and W. Sandhas, JINR report No. E4-6688 (1972).
- [7] T. W. Phillips, B. L. Berman, and J. D. Seagrave, Phys. Rev. C **22**, 384 (1980).
- [8] F. Cieselski, J. Carbonell, and C. Gignoux, Phys. Lett. **B447**, 199 (1999); J. Carbonell, Few-Body Syst. Suppl. **12**, 439 (2000).
- [9] O. A. Yakubovsky, Yad. Fiz. **5**, 1312 (1967) [Sov. J. Nucl.

| | $I \leq 1$ | $I \leq 2$ | $I \leq 3$ | $I \leq 4$ | $I \leq 5$ | $I \leq 6$ | Other work: Refs. [10, 29, 30, 31] |
|---------|------------|------------|------------|------------|------------|------------|------------------------------------|
| AV8' | 23.08 | 25.16 | 25.69 | 25.85 | 25.90 | 25.91 | 25.90 - 25.94 |
| AV18 | 22.30 | 23.75 | 24.15 | 24.20 | 24.23 | 24.24 | 24.22 - 24.25 |
| CD Bonn | 25.03 | 25.95 | 26.07 | 26.10 | 26.11 | 26.11 | 26.13 - 26.16 |
| INOY04 | 28.68 | 29.09 | 29.10 | 29.11 | 29.11 | 29.11 | 29.11 |

TABLE VII: ${}^4\text{He}$ Binding Energy (MeV) for increasing number of $2N$ partial waves characterized by maximal total angular momentum I .

| | $L = 0, S = 0$ | $L = 1, S = 0$ | $L = 2, S = 0$ | $L = 0, S = 1$ | $L = 1, S = 1$ | $L = 2, S = 1$ |
|-----------------|----------------|----------------|----------------|----------------|----------------|----------------|
| $E_n = 2.0$ MeV | 50.93 | 17.19 | -0.37 | -45.65 | 22.56 | -0.57 |
| Ref. [32] | 51.1 | 17.2 | -0.37 | -45.8 | 22.6 | -0.58 |
| $E_n = 3.5$ MeV | -64.53 | 28.00 | -1.39 | -58.17 | 40.51 | -0.94 |
| Ref. [32] | -64.6 | 28.0 | -1.40 | -58.2 | 40.5 | -0.89 |
| $E_n = 5.0$ MeV | -74.33 | 34.06 | -2.17 | -67.30 | 50.56 | -1.53 |
| Ref. [32] | -74.4 | 34.0 | -2.24 | -67.4 | 50.5 | -1.59 |

TABLE VIII: $n-{}^3\text{H}$ phase shifts at different neutron lab energies for the Malfliet-Tjon potential.

| N_k | $0^+ ({}^1S_0)$ | $0^- ({}^3P_0)$ | $1^+ ({}^3S_1)$ | $1^- ({}^3P_1)$ | $1^- ({}^1P_1)$ | $1^- (\epsilon)$ | $2^- ({}^3P_2)$ | σ_t |
|-------|-----------------|-----------------|-----------------|-----------------|-----------------|------------------|-----------------|------------|
| 14 | -70.03 | 23.78 | -62.01 | 43.49 | 22.35 | -44.58 | 46.93 | 2.290 |
| 15 | -69.57 | 23.57 | -61.61 | 43.64 | 22.40 | -44.72 | 47.18 | 2.292 |
| 16 | -69.43 | 23.51 | -61.51 | 43.63 | 22.38 | -44.75 | 47.19 | 2.290 |
| 18 | -69.72 | 23.66 | -61.76 | 43.55 | 22.39 | -44.67 | 47.03 | 2.289 |
| 20 | -69.63 | 23.62 | -61.69 | 43.54 | 22.38 | -44.69 | 47.03 | 2.288 |
| 22 | -69.68 | 23.64 | -61.73 | 43.53 | 22.39 | -44.68 | 47.01 | 2.288 |
| 24 | -69.66 | 23.64 | -61.73 | 43.53 | 22.39 | -44.68 | 47.00 | 2.288 |
| 25 | -69.67 | 23.64 | -61.73 | 43.53 | 22.39 | -44.68 | 47.00 | 2.288 |

TABLE IX: $n-{}^3\text{H}$ phase shifts, 1^- mixing parameter ϵ , and the total cross section σ_t at $E_n = 4$ MeV for increasing number of meshpoints N_k for the momenta k_x , k_y , and k_z . The $2N$ potential is AV18.

Phys. **5**, 937 (1967)].

[10] R. Lazauskas and J. Carbonell, Phys. Rev. C **70**, 044002 (2004).

[11] R. Lazauskas, J. Carbonell, A. C. Fonseca, M. Viviani, A. Kievsky, and S. Rosati, Phys. Rev. C **71**, 034004 (2005).

[12] J. A. Tjon, Phys. Lett. **B56**, 217 (1975).

[13] M. Viviani, S. Rosati, and A. Kievsky, Phys. Rev. Lett. **81**, 1580 (1998).

[14] M. Viviani, A. Kievsky, S. Rosati, E. A. George, and L. D. Knutson, Phys. Rev. Lett. **86**, 3739 (2001).

[15] A. Deltuva, A. C. Fonseca, and P. U. Sauer, Phys. Rev. C **71**, 054005 (2005).

[16] A. Deltuva, A. C. Fonseca, and P. U. Sauer, Phys. Rev. Lett. **95**, 092301 (2005).

[17] A. Deltuva, A. C. Fonseca, and P. U. Sauer, Phys. Rev. C **72**, 054004 (2005).

[18] A. Deltuva and A. C. Fonseca, in *Proceedings of the 18th International IUPAP Conference on Few-Body Problems in Physics*, Santos, 2006, nucl-th/0611013.

[19] A. C. Fonseca, in *Models and Methods in Few-Body Physics*, Lecture Notes in Physics **273**, p. 161, edited by L. S. Fereira, A. C. Fonseca, and L. Streit (Springer Verlag, Heidelberg, 1987).

[20] H. Kamada and W. Glöckle, Nucl. Phys. **A548**, 205 (1992).

[21] W. Glöckle and H. Kamada, Phys. Rev. Lett. **71**, 971 (1993).

[22] G. A. Baker, *Essentials of Padé Approximants* (Academic Press, New York, 1975).

[23] K. Chmielewski, A. Deltuva, A. C. Fonseca, S. Nemoto, and P. U. Sauer, Phys. Rev. C **67**, 014002 (2003).

[24] A. Deltuva, Ph.D. thesis, University of Hannover, 2003, <http://edok01.tib.uni-hannover.de/edoks/e01dh03/374454701.pdf>.

[25] A. Deltuva, K. Chmielewski, and P. U. Sauer, Phys. Rev. C **67**, 034001 (2003).

[26] C. de Boor, *A Practical Guide to Splines* (Springer Verlag, New York, 1978).

[27] W. Glöckle, G. Hasberg, and A. R. Neghabian, Z. Phys. **A305**, 217 (1982).

[28] W. H. Press, B. P. Flannery, S. A. Teukolsky, and W. T. Vetterling, *Numerical Recipes* (Cambridge University Press, Cambridge, 1989).

[29] A. Nogga, H. Kamada, W. Glöckle, and B. R. Barrett, Phys. Rev. C **65**, 054003 (2002).

- [30] H. Kamada *et al.*, Phys. Rev. C **64**, 044001 (2001).
- [31] M. Viviani, L. E. Marcucci, S. Rosati, A. Kievsky, and L. Girlanda, Few-Body Syst. **39**, 159 (2006).
- [32] R. Lazauskas, Ph.D. thesis, University of Grenoble, 2003; private communication.
- [33] R. B. Wiringa, V. G. J. Stoks, and R. Schiavilla, Phys. Rev. C **51**, 38 (1995).
- [34] R. Machleidt, Phys. Rev. C **63**, 024001 (2001).
- [35] V. G. J. Stoks, R. A. M. Klomp, C. P. F. Terheggen, and J. J. de Swart, Phys. Rev. C **49**, 2950 (1994).
- [36] P. Doleschall, Phys. Rev. C **69**, 054001 (2004); private communication.
- [37] D. R. Entem and R. Machleidt, Phys. Rev. C **68**, 041001(R) (2003).
- [38] J. D. Seagrave, B. L. Berman, and T. W. Phillips, Phys. Lett. **B91**, 200 (1980).
- [39] H. Rauch, D. Tuppinger, H. Wölwitsch, and T. Wroblewski, Phys. Lett. **B165**, 39 (1985).
- [40] G. M. Hale, D. C. Dodder, J. D. Seagrave, B. L. Berman, and T. W. Phillips, Phys. Rev. C **42**, 438 (1990).
- [41] J. D. Seagrave, L. Cranberg, and J. E. Simmons, Phys. Rev. **119**, 1981 (1960).
- [42] W. Tornow, H. Witała, and A. Kievsky, Phys. Rev. C **57**, 555 (1998).
- [43] V. Stoks and J. J. de Swart, Phys. Rev. C **47**, 761 (1993).